



HAL
open science

Adaptive trade-offs between vertebrate defense and insect predation drive ant venom evolution

Axel Touchard, Samuel D Robinson, Hadrien Lalagüe, Steven Ascoët, Arnaud Billet, Alain Dejean, Nathan J Téné, Frédéric Petitclerc, Valérie Troispoux, Michel Treilhou, et al.

► To cite this version:

Axel Touchard, Samuel D Robinson, Hadrien Lalagüe, Steven Ascoët, Arnaud Billet, et al.. Adaptive trade-offs between vertebrate defense and insect predation drive ant venom evolution. 2024. hal-04664882

HAL Id: hal-04664882

<https://hal.inrae.fr/hal-04664882v1>

Preprint submitted on 30 Jul 2024

HAL is a multi-disciplinary open access archive for the deposit and dissemination of scientific research documents, whether they are published or not. The documents may come from teaching and research institutions in France or abroad, or from public or private research centers.

L'archive ouverte pluridisciplinaire **HAL**, est destinée au dépôt et à la diffusion de documents scientifiques de niveau recherche, publiés ou non, émanant des établissements d'enseignement et de recherche français ou étrangers, des laboratoires publics ou privés.

1 Adaptive trade-offs between vertebrate 2 defense and insect predation drive ant venom 3 evolution

4
5 Axel Touchard^{1,2,*}, Samuel D. Robinson³, Hadrien Lalagüe¹, Steven Ascoët⁴, Arnaud Billet⁴,
6 Alain Dejean^{1,5}, Nathan J. Téné⁴, Frédéric Petitclerc¹, Valérie Troispoux⁶, Michel Treilhou⁴,
7 Elsa Bonnafé⁴, Irina Vetter^{3,7}, Joel Vizueta⁸, Corrie S. Moreau², Jérôme Orivel^{1,†}, Niklas
8 Tysklind^{6,†}

9
10
11 ¹CNRS, UMR Ecologie des forêts de Guyane – EcoFoG (AgroParisTech, CIRAD, INRAE, Université
12 de Guyane, Université des Antilles), Campus Agronomique, BP 316, 97379 Kourou Cedex, France.

13 ²Department of Entomology, Cornell University, Ithaca, New York, USA.

14 ³Institute for Molecular Bioscience, The University of Queensland, QLD 4072, Australia.

15 ⁴Equipe BTSB-EA 7417, Université de Toulouse, Institut national universitaire Jean-François
16 Champollion, Place de Verdun, 81012, Albi, France.

17 ⁵Centre de Recherche sur la Biodiversité et l'Environnement, Université de Toulouse, CNRS, Toulouse
18 INP, Université Toulouse 3 – Paul Sabatier (UPS), Toulouse, France.

19 ⁶INRAE, UMR Ecologie des forêts de Guyane - EcoFoG (AgroParisTech, CIRAD, CNRS, Université
20 de Guyane, Université des Antilles), Campus Agronomique, BP 316, 97379 Kourou Cedex, France.

21 ⁷School of Pharmacy, The University of Queensland, Woolloongabba, QLD 4102, Australia.

22 ⁸Villum Centre for Biodiversity Genomics, Section for Ecology and Evolution, Department of Biology,
23 University of Copenhagen, Copenhagen, Denmark.

24

25 *Corresponding author. Email: axel.touchard2@gmail.com (A.T.)

26 †These authors contributed equally to this work.

27

28 **Keywords:** Hymenoptera; Formicidae; Sting; Neurotoxin; Cytotoxic peptide; Defensive traits

29 **Significance**

30 Venoms are under severe evolutionary pressures, exerted either on the innovation of toxins or
31 the reduction of the metabolic cost of production (1). To reduce the metabolic costs associated with
32 venom secretion, some venomous animals can regulate venom expenditure by metering the amount of
33 venom injected and by switching between offensive and defensive compositions (2–4). Many ants use
34 venom for subduing a wide range of arthropod prey, as well as for defensive purposes against
35 invertebrates and vertebrates, but are unable to adapt venom composition to stimuli (5, 6). Consequently,
36 the expression of venom genes directly affects the ability of ants to interact with the biotic environment,
37 and the venom composition may be fine-tuned to the ecology of each species. A previous study showed
38 that defensive traits in ants exhibit an evolutionary trade-off in which the presence of a sting is negatively
39 correlated with several other defensive traits, further supporting that trade-offs in defensive traits
40 significantly constrain trait evolution and influence species diversification in ants (7). However, the sting
41 is not used for the same purpose depending on the ant species. Our study supports an evolutionary trade-
42 off between the ability of venom to deter vertebrates and to paralyze insects which are correlated with
43 different life history strategies among Formicidae.

44 **Abstract**

45 Stinging ants have diversified into various ecological niches, and several evolutionary drivers
46 may have contributed to shape the composition of their venom. To comprehend the drivers underlying
47 venom variation in ants, we selected 15 Neotropical species and recorded a range of traits, including
48 ecology, morphology, and venom bioactivity. Principal component analysis of both morphological and
49 venom bioactivity traits revealed that stinging ants display two functional strategies. Additionally,
50 phylogenetic comparative analysis indicated that venom function (predatory, defensive, or both) and
51 mandible morphology significantly correlate with venom bioactivity and amount, while pain-inducing
52 activity trades off with insect paralysis. Further analysis of the venom biochemistry of the 15 species
53 revealed switches between cytotoxic and neurotoxic venom compositions in some species. This study
54 highlights the fact that ant venoms are not homogenous, and for some species, there are major shifts in
55 venom composition associated with the diversification of venom ecological functions.

56 **Introduction**

57 Most ants secrete venom, the composition of which can vary considerably among lineages; some
58 species have formic acid or alkaloid-based venoms, while the venoms of most stinging species are
59 peptidic (8). The Formicidae have radiated into diverse ecological niches (9), and numerous
60 evolutionary forces may have contributed to the shaping of their venoms.

61 Diet is often a potent driver of venom evolution in predatory organisms (1). Many predatory
62 ants use their venom to capture a diversity of prey; however, several species or lineages are stenophagous
63 (i.e. prey exclusively on a restricted group of arthropods) (10). As most stinging ants also use their
64 mandibles to subdue their prey before delivering the paralyzing sting, mandible shape varies widely,
65 which could be a putative driver of venom composition. The morphology of the mandibles of some
66 predatory ants is indeed specialized to the shape of the prey (10, 11), while trap-jaw ants use spring-
67 loaded mandibles that snap shut on prey with high speed and force (12). Foraging activities of predatory
68 ants also range broadly from subterranean to canopy habitats, and previous research on ponerine ants
69 suggests that arboreal constraints may influence the efficacy of venom in capturing prey (13). Other ants
70 that live in mutualistic association with myrmecophytes (e.g. acacia ants) use their venom not for
71 predation, but for fierce protection of the host plant (14), while in striking contrast, some stinging species

72 lack aggression toward potential predators (15). These non-aggressive ants exhibit thanatosis (i.e.
73 feigning death) (16), escape behavior (17), or rely on morphological attributes such as spines as a
74 deterrent rather than using their sting against vertebrate predators (7). Among different lineages of
75 stinging ants, venoms can exhibit very different peptide toxin profiles (18, 19), presumably in response
76 to distinct ecological pressures. To date, no studies have integrated ecological traits, biochemical
77 composition, and bioactivity in a phylogenetic framework to explore the factors that lead to distinct
78 venom compositions in ants and, more broadly, very few in other venomous lineages (20).

79 To understand the potential evolutionary drivers underpinning stinging ant venom composition,
80 we designed a phylogenetically nested sampling of 15 Neotropical species with contrasted ecological
81 traits. Foraging activity (arboreal vs. terrestrial), venom function (predatory, defensive, both), mandible
82 morphology (trap-jaw vs. normal), and prey specialization were included as ecological factors that may
83 influence venom composition in ants. The effect of ecological traits was tested in six genera of stinging
84 ants (i.e. *Anochetus*, *Daceton*, *Neoponera*, *Odontomachus*, *Paraponera*, and *Pseudomyrmex*). The
85 genera *Neoponera*, *Odontomachus*, and *Pseudomyrmex* included both arboreal and terrestrial species to
86 assess the effect of habitat on venom composition. *Neoponera commutata* is a known specialized termite
87 predator (21). *Anochetus emarginatus* is also suspected to be a termite specialist (22, 23). The inclusion
88 of *D. armigerum* allowed testing the convergent effects of trap-jaw mandibles on venom evolution with
89 the genera *Odontomachus* and *Anochetus* (12). Within the genus *Pseudomyrmex*, we used ground-
90 dwelling (*P. termitarius*) and arboreal (*P. gracilis*) predatory species and compared them with obligate
91 plant-ant species (*P. viduus* and *P. penetrator*), which never use their venoms for predation (24), to
92 examine the effects of relaxed selection pressures for predatory capacity on venom diversity.
93 *Paraponera clavata*, notable for its painful defensive sting (25), has also been included in this panel as
94 a venom that has evolved to effectively repel vertebrate predators. We analyzed behavior, diet, a suite
95 of morphological traits, venom efficacy, and venom composition across phylogenetic relationships.

96 Results and Discussion

97 Ecological and venom-related traits

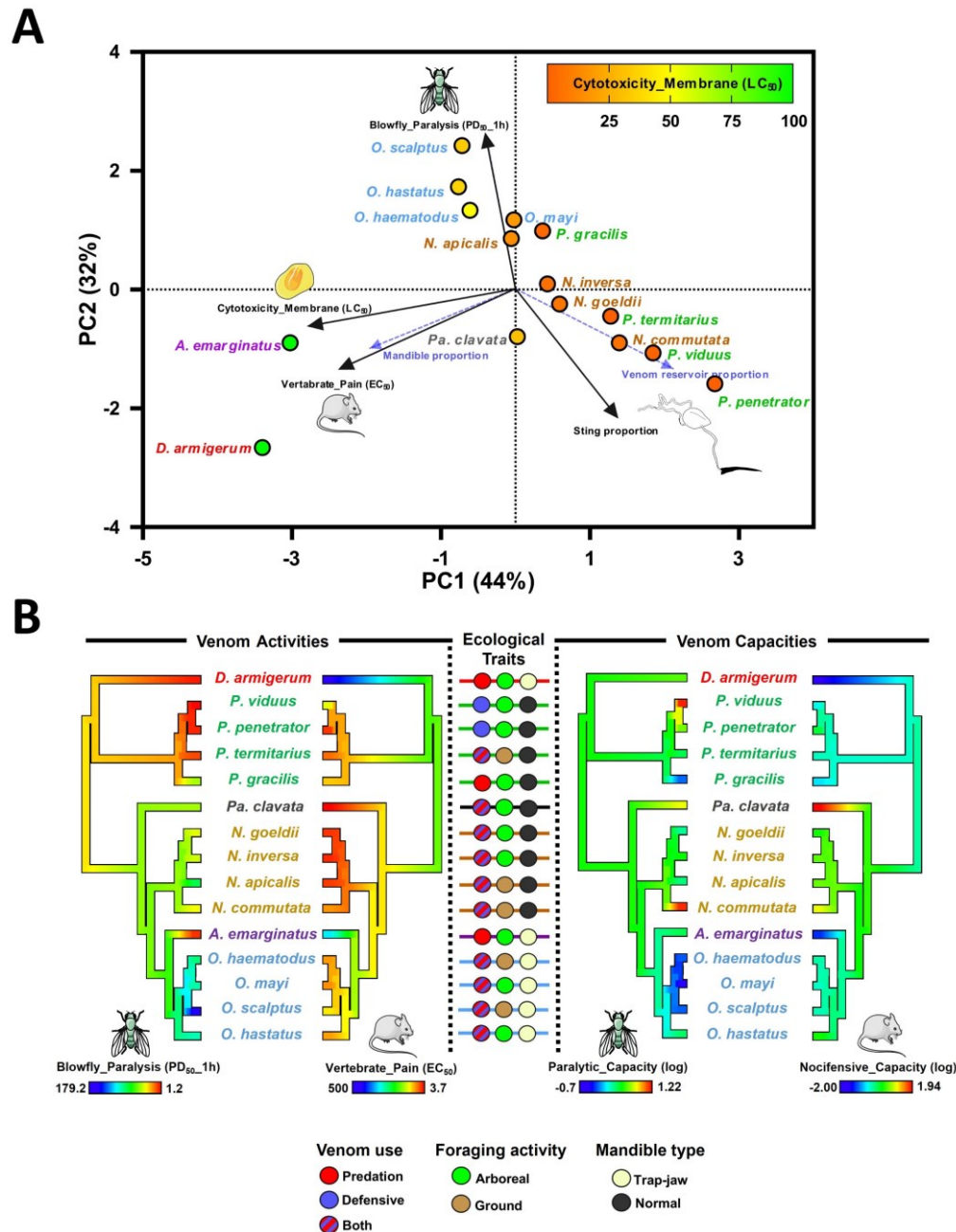
98 First, we collected observational data about the diet and the use of venom during prey capture
99 or defense to fill the ecological knowledge gap for the studied species. These observations enabled us
100 to define the ecological traits of all the species studied (**Figure 1**). We did not retain diet specialization
101 as an ecological trait for further analysis since *A. emarginatus* appeared to be an euryphagous predator
102 (i.e. prey on numerous classes of invertebrates) (*SI Appendix, Figure S1*) like all other predatory species
103 included in our study, except for *N. commutata*. We then measured how venom-related traits varied
104 among the 15 ant species (*SI Appendix, Figure S2, S3, and S4*). All the morphological data and
105 proportions related to venom yield, venom reservoir volume, sting length, and mandibles length are
106 presented in *SI Appendix, Table S1*. All studied ants use either the sting, the mandibles or both to
107 capture prey or to defend against predators. We therefore measured the proportions of the sting and the
108 mandibles with the hypotheses that a long sting would be associated with a defensive function, while
109 long mandibles would allow better seizing of prey. *Pseudomyrmex penetrator* and *Pa. clavata* had the
110 longest stings with ratios of 0.58 and 0.55 and *Odontomachus* spp., *A. emarginatus*, and *P. gracilis* the
111 shortest (ratios ranged from 0.32 to 0.41) (*SI Appendix, Figure S2, E, Table S1*). *Pa. clavata* and *D.*
112 *armigerum* were the species with the longest mandibles with ratios of 1.0 and 1.1, while *P. penetrator*,
113 *P. viduus* and *P. gracilis* have short mandibles with an average ratio of 0.4 (*SI Appendix, Figure S2, F,*
114 **Table S1**). We also evaluated the potency of the 15 venoms to trigger nociception in vertebrates and to
115 paralyze and to kill invertebrate prey (*SI Appendix, Table S2 and Table S3*). The capacity of the venom

116 of a given species is a product of both the venom potency and the amount of venom delivered. To be
117 able to compare species, we therefore calculated both their nocifensive capacity (pain-inducing) and
118 paralytic capacity by dividing the average venom yield (μg) by venom potency ($\mu\text{g}/\text{mL}$) (**SI Appendix,**
119 **Table S2 and S3**). Finally, to provide insights into the mechanism of action of the venoms, we evaluated
120 their cytotoxicity against *Drosophila* S2 cells using two assays that measure the effect on cell
121 metabolism and membrane cell integrity. At a concentration of 100 $\mu\text{g}/\text{mL}$, all crude venoms except
122 those of *A. emarginatus* and *D. armigerum* were cytotoxic (**SI Appendix, Figure S5**). The venoms of
123 *Odontomachus* spp. were cytotoxic at high doses, affecting cell metabolism with LC_{50} values ranging
124 from 15.8 to 42.9 $\mu\text{g}/\text{mL}$ and cell membranes with LC_{50} values ranging from 18.5 to 49.0 $\mu\text{g}/\text{mL}$. The
125 venoms of *Neoponera* spp. were more cytotoxic with LC_{50} ranging from 5.5 to 8.3 $\mu\text{g}/\text{mL}$ and from 5.8
126 to 14.8 $\mu\text{g}/\text{mL}$ for cell metabolism and cell membrane integrity assays, respectively. The *Pseudomyrmex*
127 spp. venoms were very cytotoxic, and the venoms of *P. penetrator* and *P. termitarius* were the most
128 potent, impacting both cell metabolism (LC_{50} of 0.05 and 0.24 $\mu\text{g}/\text{mL}$ for *P. penetrator* and *P.*
129 *termitarius*) and cell membrane integrity (LC_{50} of 0.08 and 0.23 $\mu\text{g}/\text{mL}$ for *P. penetrator* and *P.*
130 *termitarius*). *Paraponera clavata* venom was cytotoxic but was more potent on cell metabolism (LC_{50}
131 of 2.72 $\mu\text{g}/\text{mL}$) than on cell membrane integrity (LC_{50} of 31.03 $\mu\text{g}/\text{mL}$). Detailed results are presented
132 in **SI Appendix, Table S4 and Figure S5**. Since no cytotoxic activity was observed for *A. emarginatus*
133 and *D. armigerum* crude venoms, we tested the effects of these venoms on cell membrane potential on
134 S2 cells. A significant decrease in KCl-induced membrane depolarization was observed after incubation
135 with both venoms, indicating an inhibition effect on ionic conductance **SI Appendix, Figure S6**.

136 **Venom-related traits reveals the evolution of two functional strategies**

137 A principal component analysis (PCA) was done on the dataset featuring the venom activities,
138 cytotoxicity, and morphological traits. The first two axes of the PCA accounted for 76% of the total
139 variation, with axes 1 and 2 explaining 44% and 32% of the total variation, respectively (**Figure 1A**).
140 The vertebrate pain activity and insect cell cytotoxicity have significant loading on PC1 while prey
141 paralysis and sting proportion have significant loading on PC2. PCA revealed that two different venom
142 strategies are used by the studied ant species. The strategy used by *A. emarginatus* and *D. armigerum*
143 can be defined as species with a non-cytotoxic venom that is capable of paralyzing blowflies efficiently
144 but has a poor capacity to induce pain in vertebrates. All other species with the second strategy are
145 distributed along a venom cytotoxicity gradient, with the most cytotoxic venoms causing more pain in
146 vertebrates, paralysis and lethality in flies, and tending to have a longer sting.

147 Among ponerine species, we noted a major shift in insect paralytic activity with *A. emarginatus*,
148 whose venom is 13 to 22 times more paralytic than those of *Odontomachus* species and at least 5 times
149 more paralytic than those of *Neoponera* species (**Figure 1B**). Reconstruction of the ancestral state of
150 vertebrate pain activity illustrates how the venoms of *D. armigerum* and *A. emarginatus* lack vertebrate
151 pain-inducing ability (e.g. the venom of *A. emarginatus* is 3 to 5 times less active on vertebrate sensory
152 neurons than that of *Odontomachus* species and 100 times less than that of *Pa. clavata*). The amount of
153 venom varies greatly among species, which greatly impacts their paralytic and nocifensive capacities. It
154 is therefore worth noting that the venom of *A. emarginatus* and *D. armigerum* has a very low nocifensive
155 capacity, whereas the venom of *Pa. clavata* and to a lesser extent *N. commutata*, has a high nocifensive
156 capacity (**Figure 1B**).



157
 158 **Figure 1. Venom bioactivity and morphological traits in 15 ant species.** A) Principal component analysis of 15
 159 ant species defined by venom bioactivities and morphological features. PCA revealed two functional strategies
 160 among species based on the cytotoxicity of venom. The significance of each PC axis, and of loading of each trait
 161 have been tested by the PCat est R package (26). Traits having significant loadings on PC 1 and PC 2 are
 162 represented with black arrows, while others are represented with dashed blue arrows. Plot points are colored in a
 163 gradient based on membrane cytotoxicity values (LD_{50}) as indicated by the scale bar at the top right. See also *SI*
 164 *Appendix, Figure S7* for PCA on the dataset featuring all traits. B) Ancestral state reconstructions of the insect
 165 paralytic activity (PD_{50_1h}), vertebrate pain activity (EC_{50}), paralytic capacity, and nocifensive capacity of crude
 166 ant venoms, estimated by using the Phytools R package (27). Since *D. armigerum* venom was inactive on F11
 167 cells, we used an arbitrary high value of 500 $\mu\text{g}/\text{mL}$ for vertebrate pain (EC_{50}). Capacities were calculated by
 168 dividing the average venom yield (μg) by the venom potency to paralyze blowfly (PD_{50_1h} , $\mu\text{g}/\text{g}$) and to cause
 169 pain (EC_{50} , $\mu\text{g}/\text{mL}$). Venom capacities have been log-transformed. The scale bar indicates trait values from low
 170 (cool colors) to high potencies (warm colors) for venom activities and from low (cool colors) to high venom
 171 capacities (warm colors). The phylogenetic tree was reconstructed by using transcript sequences of 566 BUSCO
 172 genes expressed in the body of ant species.

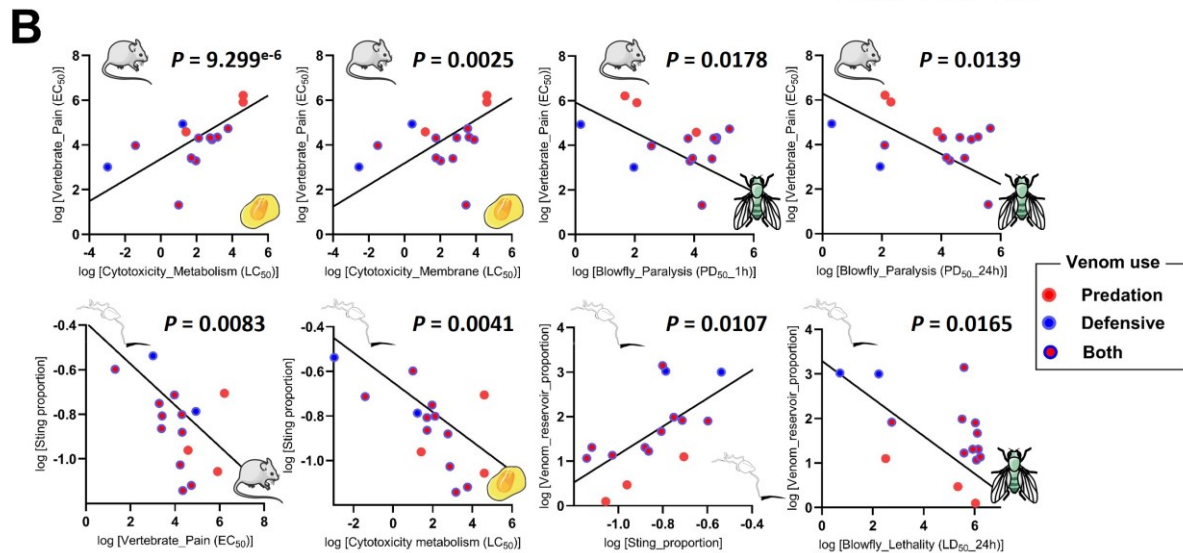
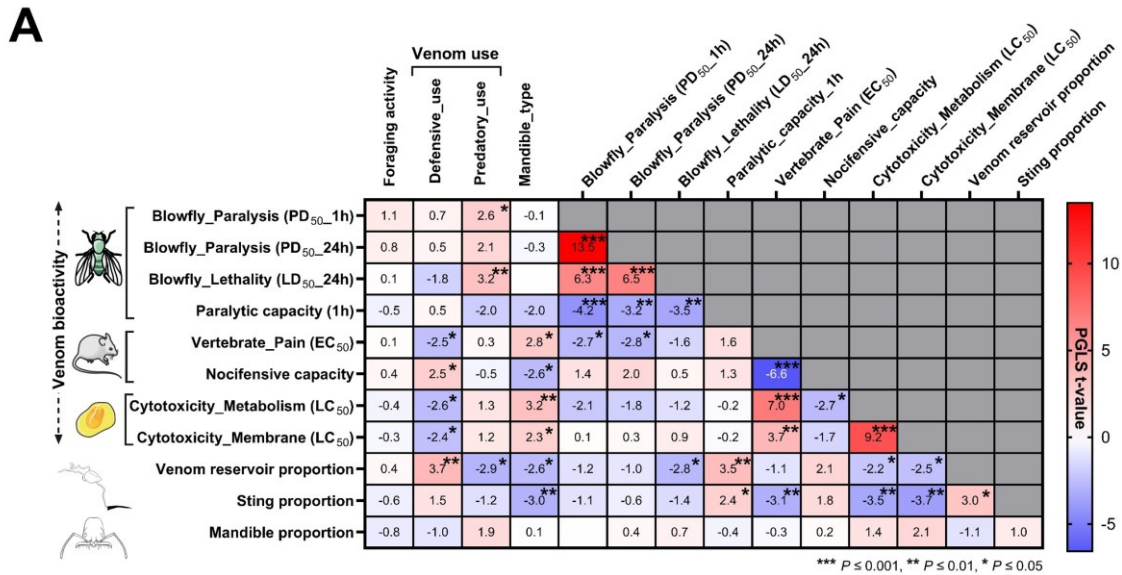
173 Altogether, the venom activities and capacities align well with the lifestyle and the venom use
174 of each species. *Anochetus emarginatus* rarely stings defensively, and the sting is not painful, causing
175 only a slight itch (personal observation A.T.) which may explain the cryptic lifestyle of most *Anochetus*
176 species (28). When disturbed, *A. emarginatus* primarily utilizes its trap-jaw mandibles to bite and
177 bounce off intruders (personal observation A.T. and (29)). *Daceton armigerum* does not sting
178 defensively (personal observation A.T.) and we showed that the crude venom caused no pain-inducing
179 activity. To avoid predation, *D. armigerum* has a very thick cuticle covered with thoracic spines and has
180 adopted an arboreal lifestyle, living in polydomous nests sheltered in hollow branches (30, 31). The
181 defensive constraint against vertebrates in *Pa. clavata* and *N. commutata* may be more pronounced than
182 in other species, since they ranked first and second in nocifensive capacity. Because of the large size of
183 workers, they nest directly in the ground, making the colony attractive in terms of nutritional resources
184 and highly vulnerable to vertebrate predation. Among ponerine ants, the venom of *Odontomachus* spp.
185 has a low paralytic activity and capacity. *Odontomachus* spp. capture their prey with trap-jaw mandibles
186 and do not always use their venom, depending on the prey type (32). In the *Pseudomyrmex* clade, the
187 venom of the plant-ant species (i.e. *P. penetrator* and *P. viduus*) has a very high paralytic capacity on
188 insects, in marked contrast to that of *P. gracilis*. Although *P. viduus* and *P. penetrator* species do not
189 use their venom for predation, they are subject to strong selective pressures to defend host plants against
190 both grazing insects and vertebrates. *Pseudomyrmex penetrator* venom is also highly effective at
191 inducing pain in vertebrates (**SI Appendix, Tables S2**).

192 **Correlation among traits**

193 Comparative phylogenetic generalized least squares (PGLS) regression revealed several
194 significant correlations among traits (**Figure 2**). For the evolutionary impact of ecological traits, we
195 found that both venom use and mandible type significantly correlate with venom bioactivities and
196 morphological traits, while there is no correlation between foraging activity (arboreal vs. terrestrial-
197 foraging species) and any other traits (**Figure 2A**). We show that the metabolic cost of toxin secretion
198 is reduced in stinging ant species with relaxed selective pressure for defensive function, since they
199 produce less venom than other ants (proportion of venom reservoir volume ($P = 0.003$)). The defensive
200 function significantly affects the properties of venom: the venoms of species that use their venom
201 defensively generally have greater cytotoxicity (cytotoxicity_metabolism, $P = 0.021$;
202 cytotoxicity_membrane, $P = 0.031$), as well as greater vertebrate pain activity ($P = 0.03$), associated
203 with higher nocifensive capacity ($P = 0.03$) than species that use venom exclusively for predatory
204 purposes. Counterintuitively, the predatory use of venom significantly reduces the potency against prey,
205 measured as paralysis ($P = 0.024$) and lethality ($P = 0.007$) in blowflies, suggesting that some predatory
206 species may compensate low venom activity to capture prey with other adaptations such as trap-jaw
207 mandibles. Mandible strike performances vary among trap-jaw species and may however have a variable
208 influence on the venom activity (33). In this study, the presence of trap-jaw mandibles has no effect on
209 venom activity against blowflies, both paralysis and lethality, but was correlated with low vertebrate
210 pain activity ($P = 0.016$), low venom volume ($P = 0.022$), a smaller sting ($P = 0.010$), low nocifensive
211 capacity ($P = 0.021$), and low cytotoxicity (cytotoxicity_metabolism, $P = 0.007$;
212 cytotoxicity_membrane, $P = 0.036$). The presence of specialized mandibles is therefore associated with
213 an overall decrease in the defensive function of venom.

214 The data showed that the longer the sting, the more pain activity ($P = 0.008$) and cytotoxicity
215 (cytotoxicity_metabolism, $P = 0.004$; cytotoxicity_membrane, $P = 0.002$) were found in the venom,
216 which is consistent with an anti-vertebrate role for a long sting. PGLS regression showed a significant
217 positive correlation between the venom reservoir proportion with both the sting proportion and lethality
218 in blowflies ($P = 0.011$). Pain activity in vertebrates is strongly positively correlated with the

219 cytotoxicity of venoms (cytotoxicity_metabolism, $P < 0.001$; cytotoxicity_membrane, $P = 0.002$) but
 220 negatively correlated with the paralysis in blowflies (blowfly_paralysis_1h, $P = 0.018$;
 221 blowfly_paralysis_24h, $P = 0.014$) (**Figure 2B**). This is suggestive of a trade-off between vertebrate
 222 pain-inducing activity and insect-predation activity in these ant venoms. Such a trade-off might translate
 223 to life history strategies, where species with potent paralytic venom against prey have reduced capacity
 224 to deter vertebrate predators and are therefore prone to adopt alternative defensive strategies, such as
 225 cryptic habits, nesting strategies (e.g. polydomous nest) or promoting behavioral (e.g. thanatosis or
 226 escape behavior) and morphological (e.g. thick cuticle and spines; body size reduction) anti-predation
 227 co-adaptations.



228
 229 **Figure 2. Comparative phylogenetic analysis.** A) Phylogenetic generalized least squares (PGLS) analysis among
 230 ecological traits, venom bioactivity, and morphological traits in the 15 ant species. As “venom use” is a multi-state
 231 discrete variable with non-ordinal properties that contain a category “both”, we decomposed that trait into two
 232 binary discrete variables (defensive_use and predatory_use) having only two states (yes or no). Heatmap with
 233 PGLS t-values and statistical significance. Positively correlated values are in red and negatively correlated values
 234 are in blue. B) PGLS linear regressions of several significantly correlated traits.

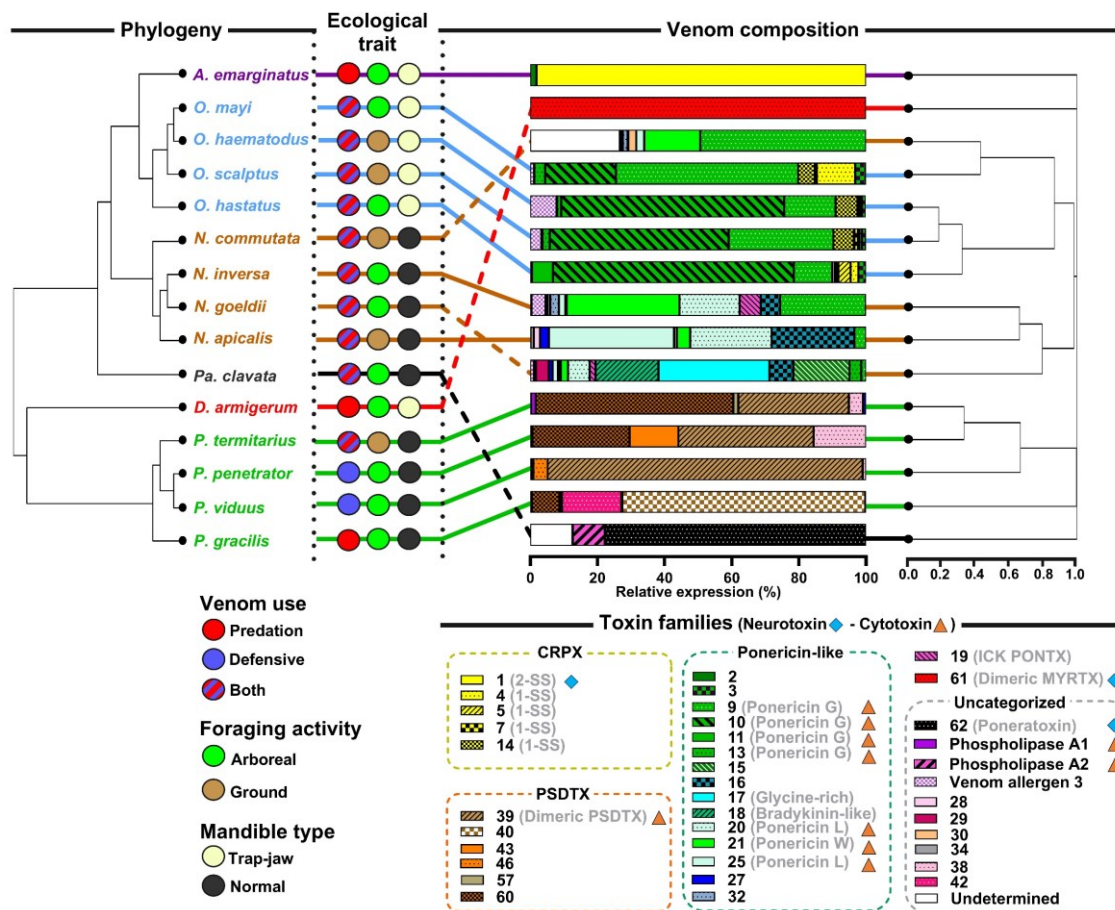
235 The venom composition of stinging ants

236 To understand the biochemical mechanisms underlying the observed variations in venom
237 efficacy, we examined the venom composition of each of the 15 species (**Figure 3**). For further details
238 on venom composition, see **SI Appendix, Figures S8-S19** and **Dataset S1**. Overall, our investigations
239 revealed that the venoms displayed heterogeneity in composition, with a considerable turnover of
240 peptide families across genera and without any correlation with the ecological traits considered. Most
241 of the peptide families were genus specific with only family 9 (ponericin G) shared between
242 *Odontomachus* and *Neoponera* venoms. The venoms of the three species that were unique for their
243 genus (i.e. *Pa. clavata*, *A. emarginatus*, and *D. armigerum*) showed a very distinctive profile dominated
244 by families of neurotoxins not shared with any other venom. Our results also showed that many venom
245 peptide families are shared by species of the same genus, but the proportion varied.

246 Among the species that use their venom exclusively for predation, *A. emarginatus* and *D.*
247 *armigerum* are associated with a complete shift in venom bioactivities that correlate with a switch to a
248 neurotoxic venom composition. The venom of *D. armigerum* showed a unique profile, as previously
249 reported (18), and our analysis confirmed that this venom consists of a single family of peptides (dimeric
250 MYRTX, family 61) that display some amino acid sequence similarity with the neurotoxic U₁₁ venom
251 peptide from *Tetramorium bicarinatum* (34) (**SI Appendix, Figure S20**). Given the lack of cytotoxicity
252 but strong paralytic activity on blowflies and inhibition of cell membrane potential, these data suggest
253 that *D. armigerum* has an insect neurotoxic venom. In addition, *A. emarginatus* has a non-cytotoxic
254 venom that is much more paralytic to insects than the other ponerine venoms studied. Given the
255 dominance of family 1 peptides in *A. emarginatus* venom (98% of relative expression), it is likely that
256 2-SS CRPXs (family 1) are responsible for most, if not all, of the paralytic effects upon prey. Since one
257 of the peptides from family 1 (i.e. Ae1a) has shown inhibition (at a high concentration) on the human
258 voltage-gated calcium channel (Ca_v1), it is possible that 2-SS CRPXs are neurotoxins (35). Although
259 the venoms of *D. armigerum* and *A. emarginatus* share similar non-cytotoxic, insect neurotoxic activity,
260 the difference in composition suggests that they have evolved independently. By contrast, the stings of
261 other ponerine *Odontomachus* spp., and *Neoponera* spp. induce sharp pain (36, 37) and showed stronger
262 pain activity in our assay. Ponericins are very prevalent in the venom composition of *Odontomachus*,
263 *Neoponera*, and several other ponerine ants (37–39). Ponericins are multifunctional cytotoxic peptides
264 acting on the cell membranes (40, 41), and those from the venoms of *N. apicalis* and *N. commutata* are
265 known to cause pain in mammals and to paralyze insects (42). There is compelling evidence that
266 membrane-active venom peptides contribute to the defensive role of multiple venomous arthropods
267 against vertebrates (5, 43–45).

268 Neurotoxic peptides are not exclusive to ants that rely on venom solely for predation. The venom
269 of *Pa. clavata* is largely dominated by poneratoxin (family 62) (46), a pain-inducing neurotoxin that
270 efficiently modulates vertebrate voltage-gated sodium (Na_v) channels while paralyzing insects only at
271 very high doses (47). We showed that the venom of *Pa. clavata* also exhibits cytotoxicity, which is
272 likely attributed to phospholipase A₂ (PLA₂), present in this venom at higher levels than in other ants.
273 Since *Pa. clavata* also uses its venom for predation, cytotoxicity may also be a means of subduing
274 arthropod prey. Alternatively, cytotoxicity may also be a means of maintaining a multifunctional defense
275 against predators. In this way, the venom retains a general repellent effect that ensures a baseline defense
276 of the colony in a scenario where a predator would acquire resistance to neurotoxins. This hypothesis is
277 supported by a previous study of the venom of the seed-harvesting ant *Pogonomyrmex*, which uses its
278 venom primarily for defense against vertebrates, and has evolved venoms dominated by vertebrate-
279 selective peptides that target Na_v channels, but still contain a peptide that is cytotoxic to vertebrate cells
280 (48).

281 Our results indicated that the four *Pseudomyrmex* species have highly cytolytic venoms and
 282 different venom profiles to other ant species, with peptide families not shared with the other species
 283 studied. We found that *P. gracilis* shares few similarities with the other three *Pseudomyrmex* species,
 284 and that the different venom families are present in different proportions among the species. Among
 285 these families, family 39 corresponded to the myrmexins (renamed here the dimeric
 286 pseudomyrmeciitoxin (PSDTX)), a group of dimeric peptides first described in the venom of *P.*
 287 *triplarinus* (49) which are highly cytotoxic to insect cells (50). Dimeric PSDTXs largely dominate the
 288 venom of *P. viduus* (94% of relative venom expression), which was found to be the most paralytic and
 289 lethal venom on blowflies. The other families consist of cysteine-free polycationic peptides which may
 290 also contribute to the observed cytotoxicity. The venom of *P. penetrator* is at least 3 times more
 291 cytotoxic than in other *Pseudomyrmex*, at least 72 times more cytotoxic than *Neoponera*, and at least
 292 231 times more cytotoxic than *Odontomachus* (*SI Appendix, Table S4*). This is associated with high
 293 efficacy for inducing pain in vertebrates and paralyzing insects. This example highlights the fact that
 294 the trade-off between vertebrate and insect-predatory venom activity may be disrupted by very high
 295 cytotoxicity.



296 **Figure 3. Comparison of venom composition and phylogenetic relationships among 15 ant species.** Venom
 297 composition cladogram is based on the relative expression (TMM) of transcripts identified as toxins in each venom
 298 gland transcriptome and converted into Bray-Curtis distance matrix and hierarchical cluster analysis was
 299 performed by using the complete linkage method of `hclust()` function with the R software. Only families with a
 300 relative expression value >1% in at least one species are shown in the color key. Toxin families are grouped by
 301 precursor clades (*SI Appendix, Figure S19*). Blue diamonds and orange triangles indicate neurotoxic and cytotoxic
 302 peptide families, respectively, based on the literature. In contrast to the other species, *A. emarginatus*, *D.*
 303 *armigerum*, and *Pa. clavata* have convergently evolved a venom composition dominated by neurotoxic peptides.

305 Conclusion

306 Here we use a multi-pronged approach to test foraging activity, venom function, and mandible
307 morphology as evolutionary drivers underlying venom variation in ants. We show that ant venoms can
308 be highly heterogeneous and that there have been major shifts in venom composition and bioactivities,
309 even among phylogenetically close species. The ecological role of the venom, offensive or defensive,
310 and even more so the breadth of biological targets, is arguably the dominant constraint in the evolution
311 of stinging ant venom cocktails. Metering the amount of venom produced is the swiftest way to adapt
312 to different ecological constraints (51) such as for *N. commutata*, which has a quite similar venom
313 composition profile to other congeneric ponerine species but produces large amounts of venom.
314 Evolution may further fine-tune venom composition toward ecologically relevant cocktails exhibiting
315 different functional strategies based on either neurotoxins or cytotoxins. Cytotoxic toxins, which do not
316 require a specific pharmacological receptor, are likely to offer an evolutionary advantage to species that
317 need to target a wide range of both vertebrate and arthropod organisms with highly divergent nervous
318 systems. In some lineages of ants, however, evolution may have favored neurotoxin-based venoms as
319 the range of biological targets narrowed. A reasonable explanation for the prevalence of neurotoxic-
320 based venoms in ants would be that cytotoxic peptides often act at high concentrations compared to
321 neurotoxins (47), and are therefore likely to be associated with higher metabolic costs. Toxin innovation
322 in the venoms of the Formicidae may therefore facilitate diversification of lifestyle and morphology,
323 and ultimately contribute to speciation.

324 Material and Methods

325 Ants and venom samples preparation

326 Live specimens of worker ants from different colonies for each species were collected in French
327 Guiana. To identify genes involved in venom production, we aimed to generate whole-body (i.e. head
328 and thorax) and venom gland transcriptomes for each species, and then, subtract genes expressed in the
329 whole-body transcriptome from those in the venom gland, to identify those genes expressed largely in
330 venom glands. For each species we dissected: 1) both venom glands and venom reservoirs from 100 live
331 workers per species in ultrapure water and immediately placed in 1 mL of RNAlater™ (Thermo Fisher
332 Scientific, Waltham, MA, USA); and 2) the head and thorax of 2-3 workers in 1 mL of RNAlater™.
333 Samples were stored at -80°C prior to RNA extraction. Crude venom samples were prepared by
334 dissecting ant venom reservoirs in ultrapure water, then pooled in 10% acetonitrile (ACN) in ultrapure
335 water and stored at -20°C prior to freeze-drying. Venom samples were then loaded onto a $0.45\ \mu\text{m}$
336 Costar® Spin-X tube filter (Corning Incorporated, Corning, NY, USA) and centrifuged at 12,000 g for
337 3 min to remove tissues from the venom apparatus. Filtered venom samples were then lyophilized,
338 accurately weighed, and stored at -20°C until further use.

339 Transcriptomics

340 The RNAlater™ was removed from the tubes containing the samples using a glass Pasteur
341 pipette. Subsequently, the glands or ant bodies (head and thorax) were then disrupted using a
342 TissueLyser II (Qiagen, Germantown, MD, USA) in RLT buffer containing 10% (v/v) of 2-
343 mercaptoethanol (Rneasy Mini Kit, Qiagen). RNA was isolated using a phenol-chloroform (5:1)
344 solution, followed by washing with chloroform-isoamyl alcohol (25:1) to remove any phenol traces. The
345 RNA was bound to a Qiagen column and washed according to the manufacturer's instructions. DNase
346 I (Roche Diagnostics GmbH, Mannheim, Germany) was added to eliminate any remaining DNA

347 fragments. The RNA was eluted using sterile water, and total RNA was quantified using a Qubit 3.0
348 fluorometer (Thermo Fisher Scientific, Waltham, MA, USA) with the RNA HS assay kit (Life
349 Technologies Corp., Carlsbad, CA, USA). A NanoDrop 2000 UV-Vis spectrophotometer (Thermo
350 Fisher Scientific) was used to determine the 260/280 and 260/230 nm ratios. Finally, the purified RNA
351 was treated with RNastable™ LD (Biomatrix, San Diego, CA, USA) and dried using a Speed Vac
352 (RC1010, Jouan, Saint Herblain, France) and sent for sequencing.

353 Sequencing

354 Samples were sent to IGA Technologies Services (Udine, Italy) where samples were suspended
355 and RIN number checked before preparation of the mRNA-seq stranded libraries. All libraries were
356 pooled and sequenced with RAPID 2 × 250 bp runs on a HiSeq2500 Illumina sequencer (480 Million
357 reads). Raw sequences were demultiplexed and used in downstream analyses. The resulting library size
358 ranged from 18.4 M to 28.3 M reads and were 22.1 M reads on average.

359 Transcriptome assembly, annotation, and quantification of gene expression

360 Recent RNA-Seq advancements offer cost-effective transcriptome data collection, yet
361 reconstructing full-length transcripts in non-model species from short reads remains challenging. A
362 cautious approach consists of testing different programs and selecting the one producing the best
363 expected de novo assembly (52). Three commonly used programs were tested: SOAPdenovo-Trans
364 v1.03 (53), maSPAdes v3.13.1 (54) and Trinity v2.6.6 (55). Before assembly, the libraries were trimmed
365 with cutadapt v2.3 (56). For the pilot run, the assemblies with the three programs were made on two
366 species, *Anochetus emarginatus* and *Pseudomyrmex gracilis*. For the latter species, a genome and
367 transcriptome were available (57). The resulting assemblies were compared with TransRate v1.01 (58),
368 BUSCO v3.0.1 and the hymenoptera_odb9 database (59), and for *P. gracilis* only, with RNAQuast v2.1
369 (60) which computes some metrics with the use of a genome of reference. Based on the results and
370 metrics obtained with the last three tools (data available on request), Trinity assembler was chosen for
371 assembling the remaining 12 species using both venom glands and bodies libraries.

372 Homologies with known proteins were searched with Blastx on the curated UniProt-SwissProt
373 database (accessed the 1st September 2019) and ToxProt database. Open reading frames (ORFs) were
374 searched with TransDecoder (61). The minimal length of the ORF was set to 10 amino acids in order to
375 keep the potential small venom peptides. Homologies of the predicted ORFs with proteins from the
376 UniProt-SwissProt database were searched with BLASTp. Additional protein information was searched
377 through the pfam database with hmmscan. The presence of rRNA was searched with Barrnap. The
378 presence signal peptide was searched with SignalP v4.1 (61, 62). The transmembrane site was searched
379 with Tmhmm v2.0 (63). Transdecoder was run again to integrate the BlastP and Pfam criteria in the
380 coding region selection. Following the Trinity procedure, venom glands and bodies libraries were
381 separately mapped and quantified using Bowtie2 (63, 64) and RSEM (65) using TMM normalization
382 method. All the annotation results were integrated in a sqlite database with Trinotate v3.2 (66).

383 Proteomics

384 LC-MS profiling of the crude venoms was carried out on the LTQ-XL equipped with an ESI-
385 LC system Vanquish (ThermoFisher Scientific, Courtaboeuf, France). Peptides were separated using an
386 Acclaim RSLC C₁₈ column (2.2 μm; 2.1 x 150 mm; ThermoFisher, France). The mobile phase was a
387 gradient prepared from 0.1% aqueous formic acid (solvent A) and 0.1% formic acid in acetonitrile
388 (solvent B). The peptides were eluted using a linear gradient from 0 to 50% of solvent B during 45 min,
389 then from 50 to 100% during 10 min, and finally held for 5 min at a 250 μL min⁻¹ flow rate. The
390 electrospray ionization mass spectrometry detection was performed in positive mode with the following

391 optimized parameters: the capillary temperature was set at 300°C, the spray voltage was +4.5 kV, and
392 the sheath gas and auxiliary gas were set at 50 and 10 psi, respectively. The acquisition range was from
393 100 to 2000 *m/z*. The area value of each peak corresponding to a peptide was manually integrated using
394 the peak ion extraction function in Xcalibur software (version 4.0, ThermoFisher Scientific,
395 Courtaboeuf, France). The relative peak area indicates the contribution of each peptide to all the peptides
396 identified in the venom, providing a measure of relative abundance.

397 For reduction/alkylation, 300 µg of crude venom was incubated with 10 µL of 100 mM
398 ammonium bicarbonate buffer (pH 8) containing 10 mM dithiothreitol (DTT) for 30 min at 56°C. After
399 reducing with DTT, the samples were alkylated by adding 10 µL of 50 mM iodoacetamide (IA) for 15
400 min at room temperature in the dark. Reduced/alkylated venoms were freeze-dried prior to shotgun
401 proteomics. The venoms were resuspended in 100 µL 10% ACN and desalted using ZipTip µ-C₁₈ Pipette
402 Tips (Pierce Biotechnology, Rockford, IL, USA). Samples were analyzed using an Orbitrap Fusion
403 equipped with an easy spray ion source and coupled to a nano-LC Proxeon 1200 (Thermo Scientific,
404 Waltham, MA, USA). Peptides were loaded with an online preconcentration method and separated by
405 chromatography using a Pepmap-RSLC C₁₈ column (0.75 x 750 mm, 2 µm, 100 Å) from Thermo
406 Scientific, equilibrated at 50°C and operating at a flow rate of 300 nL/min. Peptides were eluted by a
407 gradient of solvent A (H₂O, 0.1% FA) and solvent B (ACN/H₂O 80/20, 0.1% FA), the column was first
408 equilibrated 5 min with 95% of A, then B was raised to 28% in 105 min and to 40% in 15 min. Finally,
409 the column was washed with 95% B during 20 min and re-equilibrated at 95% A during 10 min. The
410 Advanced Peak Determination (APD) algorithm was used during the acquisition. Peptide masses were
411 analyzed in the Orbitrap cell in full ion scan mode, at a resolution of 120,000, a mass range of *m/z* 350-
412 1550 and an AGC target of 4.105. MS/MS were performed in the top speed 3 s mode. Peptides were
413 selected for fragmentation by Higher-energy C-trap Dissociation (HCD) with a Normalized Collisional
414 Energy of 27% and a dynamic exclusion of 60 s. Fragment masses were measured in an Ion trap in the
415 rapid mode, with an AGC target of 1.104. Monocharged peptides and unassigned charge states were
416 excluded from the MS/MS acquisition. The maximum ion accumulation times were set to 100 ms for
417 MS and 35 ms for MS/MS acquisitions respectively. Using PEAKS X+ Studio (Bioinformatics
418 Solutions Inc., Waterloo, ON, Canada) in no-enzyme mode, MS/MS spectra were searched against the
419 translated venom-apparatus transcriptomes. Precursor and fragment mass tolerances were set to
420 respectively 7 ppm and 0.5 Da. The following post-translational modifications were included as
421 variable: Acetyl (Protein N-term), Oxidation (M), Phosphorylation (STY), Deamidation (NQ),
422 Amidation (C-term), HexNAcylation (ST), Pyro-glu (EQ). The following post-translational
423 modifications were included as fixed: Carbamidomethyl (C). Spectra were filtered using a 1% FDR.

424 **Venom composition analysis**

425 To characterize the venom composition of each species we employed a transcriptomic approach
426 with mass spectrometry to validate the presence of peptides in the venom. From the transcriptomes
427 generated, the annotations were manually curated focusing on transcripts coding for toxins, with
428 consideration of gene expression levels in venom glands and in the body. Additionally, we selected and
429 examined additional transcripts based on precursor similarities to known toxin peptides. A total of 465
430 transcripts encoding putative toxins were retained for subsequent analysis (**SI Appendix, Figure S8** and
431 **Dataset S1**). Crude venom from all species was obtained by dissection of venom reservoirs. Venoms
432 were then reduced/alkylated and analyzed through shotgun LC-MS/MS proteomics. The PEAKS
433 software was used to analyze the mass spectrometry fragmentation spectra, with the transcriptome of
434 each species implemented as a database for peptide sequence assignment. Positive matches of
435 proteomics data with transcripts allowed us to confirm 305 peptide sequences. Total ion chromatograms
436 were also generated with crude venoms and the LC-MS profile annotated (**SI Appendix, Figure S9-10**).

437 Transcripts were classified into families based on the similarity of the amino acid sequences of the
438 mature regions. For each family, multiple alignments of full-length precursors were generated using the
439 Muscle program in MEGA-X version 10.1.8 (67) and edited using Jalview version 2.11.2.7 (68). We
440 classified the transcripts into 62 peptide families and 3 enzyme toxins (i.e. phospholipase A₁,
441 phospholipase A₂, and venom allergen 3) (**SI Appendix, Figure S11-18**). Peptide transcripts were
442 further clustered into five gene clades (i.e. cysteine-rich poneritoxin, ponericin-like,
443 pseudomyrmecitoxin (PSDTX), ICK-PONTX, dimeric myrmecitoxin (MYRTX)) according to the
444 predictive signal sequence (**SI Appendix, Figure S19**). A total of 14 toxin families (i.e. families 23, 26,
445 29, 33, 34, 35, 37, 49, 52, 54, 56, and 59) were not included in the venom composition analysis for
446 clustering because no transcript sequences could be confirmed by mass spectrometry, yet they were
447 retained in the sequence alignments. The full list of transcripts expressed in venom glands with a TMM
448 greater than 100, the identified toxin precursor sequence, the predicted mature part, the family
449 assignment, and PEAKS results can be found in **Dataset S1**. The venom composition of *Pa. clavata*,
450 previously published by Aili *et al* (46) has been included in our analysis. For venom clustering, a Bray-
451 Curtis distance matrix based on the relative expression of the toxin family was generated using the
452 `veggdist ()` function from the R package "vegan" (69), followed by hierarchical clustering analysis
453 (HCA) using the `hclust ()` function with the full method from the R package "stats" (70). The `dendlist`
454 `()` function from the R package "dendextend" (71) was used to plot and align the species phylogeny tree
455 with the venom composition HCA cladogram. The final Figure 2 was edited in GraphPad Prism v10.0.3.
456 To define gene clades, we used an approach based on similarity of signal parts. Signal parts were
457 predicted using SignalP - 6.0 server (72) and then aligned using the Muscle program in MEGA-X (67).
458 A pairwise distance matrix between sequences was extracted from the multiple alignments and used for
459 HCA clustering using the `hclust ()` function with the ward method from the R package "stats".

460 **Morphological traits**

461 Six morphological traits were measured on up to 13 randomly selected workers per species.
462 Measurements were made using an ocular micrometer accurate to 0.01 mm mounted on a Leica M80 or
463 Leica S9E stereomicroscope (Leica Microsystems, Heerbrugg, Switzerland). The traits considered were
464 Weber's length, head length, mandible length, sting length, venom reservoir length, and venom reservoir
465 width. We estimated the venom reservoir volume using the standard ellipsoid formula; $\pi/6$ (venom
466 reservoir length \times venom reservoir width²). For analysis we used size/volume-corrected ratios calculated
467 as follows: mandible proportion (mandible length / head length), sting proportion (sting length / weber's
468 length), venom reservoir proportion (venom reservoir volume / weber's length³).

469 **Neuronal cells assays**

470 F11 (mouse neuroblastoma \times DRG neuron hybrid) were maintained on Ham's F12 media
471 supplemented with 10% FBS, 100 μ M hypoxanthine, 0.4 μ M aminopterin, and 16 μ M thymidine
472 (Hybri-Max, Sigma Aldrich). 384-well imaging plates (Corning, Lowell, MA, USA) were seeded 24 h
473 prior to calcium imaging, resulting in \sim 90% confluence at the time of imaging. Cells were loaded for 30
474 min at 37°C with Calcium 4 assay component A in physiological salt solution (PSS; 140 mM NaCl, 11.5
475 mM D-glucose, 5.9 mM KCl, 1.4 mM MgCl₂, 1.2 mM NaH₂PO₄, 5 mM NaHCO₃, 1.8 mM CaCl₂, 10
476 mM HEPES) according to the manufacturer's instructions (Molecular Devices, Sunnyvale, CA). Ca²⁺
477 responses were measured using a FLIPRPenta fluorescent plate reader equipped with a CCD camera
478 (Ex: 470 to 490 nm, Em: 515 to 575 nm) (Molecular Devices, Sunnyvale, CA). Signals were read every
479 second for 10 s before, and 300 s after, the addition of venoms (in PSS supplemented with 0.1% BSA).

480 **Insect activity assays**

481 Blowfly larvae (*Lucilia caesar*) were purchased from a fisheries shop (Euroloisir81, Lescure-
482 d'Albigeois, France) and kept at 25°C until hatching. Flies 1-4 days after hatching were used for injection
483 assays. Blowfly assays were done through lateral intrathoracic injection of 1 µL of venom dissolved in
484 ultra-pure water at various concentrations using a fixed 25-gauge needle attached to an Arnold hand
485 microapplicator (Burkard Manufacturing Co., Ltd., Rickmansworth, UK) with a 1.0 mL Hamilton
486 Syringe (1000 Series Gastight, Hamilton Company, Reno, NV, USA). Then, the blowfly was placed in
487 an individual 2 mL tube containing 15 µL of 5% glucose solution. Paralysis was monitored at 1 h and
488 24 h post-injection, while lethality was monitored at 24 h. Flies that did not display any signs of
489 movement dysfunction were considered unaffected, otherwise they were recorded as paralyzed. Flies
490 were deemed dead if they did not respond at all to tweezer mechanical stimulation as observed under a
491 dissecting microscope. Ten flies were used for each toxicity experiment and for the corresponding
492 control (ultrapure water solution). Each dose was repeated three times.

493 **Cytotoxicity and membrane potential assays**

494 *Drosophila* S2 cells (ThermoFisher, USA) were maintained and prepared for cytotoxicity and
495 membrane potential variation assays as previously detailed (34, 73). Lyophilized crude venoms were
496 solubilized in ultra-pure water and diluted in culture medium before being exposed to cells at various
497 final concentrations (from 1 ng/mL to 100 µg/mL) for 24 h at 25°C for cytotoxic assays or at 100 µg/ml
498 for 30 min at 25°C for membrane potential monitoring. Cytotoxic assays were performed using lysis
499 buffer and culture medium as positive and negative controls or blanks, respectively. The assays and
500 calculations of LC₅₀ were performed as previously described (73). Membrane potential changes were
501 measured using a buffer containing: 115 mM NaCl, 5 mM KCl, 2 mM CaCl₂, 1 mM MgCl₂, 48 mM
502 sucrose, and 10 mM HEPES. The assay and analysis were performed as previously described (34).

503 **Phylogenetic analysis**

504 To generate a phylogeny of the studied species we searched for conserved genes across their
505 transcriptome assemblies, or genome for *Pa. clavata*, using BUSCO v5.1.2 (59). Using the
506 hymenoptera_odb10 database, we identified 566 genes present in at least 90 % of the species. We
507 aligned the protein sequences from each gene using mafft and concatenated them into a supermatrix
508 (**Dataset S2**). Then, we used IQTREE2 v2.1.2 (74) to reconstruct the maximum likelihood tree by using
509 the concatenated matrix and the selection of the best substitution model with ModelFinder and 1000
510 ultrafast bootstrap replicates.

511 Ancestral states reconstruction for venom activities and capacities, were estimated by maximum
512 likelihood using the contmap () function of the Phytools R package with default settings. To test for
513 statistical support for correlations between venom bioactivities and morphological traits, and the
514 influences of ecological traits, we used the phylogenetic Generalized Least Squares (PGLS) approach
515 using the PGLS () function of the "caper" package in RStudio, with the formula set as ([functional traits,
516 e.g. vertebrate_pain] ~ grouping [ecological traits, e.g. defensive_use (yes or no)] and lambda set to
517 "Maximum Likelihood". For the PGLS regressions, we treated log-transformed continuous traits.

518 **Acknowledgments**

519 We thank Wolfgang Wuster and Nicholas Casewell for valuable input into the experimental design. We
520 thank Philippe Gaucher for providing a colony of *Pseudomyrmex viduus*. We thank Federica Catonaro,
521 Elena di Barbora, and Emanuela Aleo for assistance with transcriptome library construction and

522 sequencing. This research was funded by Investissement d’Avenir grant of the Agence Nationale de la
523 Recherche (CEBA: ANR- 10-LABX-25-01) and by the PO-FEDER 2014–2020, Région Guyane
524 (FORMIC, GY0013708). Ant samples were collected under the authorizations of the French Ministry
525 of Ecological and Solidarity Transition, in accordance with Article 17, paragraph 2, of the Nagoya
526 Protocol on Access and Benefit-sharing (Reference number of the permit: TREL1916196S/214).

527 Data availability

528 The raw sequencing reads used in this manuscript are available from the National Center for
529 Biotechnology Information (NCBI) under the project code PRJNA1061791. The mass spectrometry
530 proteomics data have been deposited to the ProteomeXchange Consortium via the PRIDE partner
531 repository with the dataset identifier PXD050348.

532 Author contributions

533 A.T., J.O., and N.T. designed research; A.T., S.D.R., H.L., S.A., N.J.T., V.T., F.P., and A.B. performed
534 research; J.O., N.T., E.B., M.T., I.V., and C.S.M. contributed resources; A.T., S.D.R., and H.L. analyzed
535 data; A.T. wrote the manuscript; all authors have read and agreed to the published version of the
536 manuscript.

537

538 References

- 539 1. N. R. Casewell, W. Wüster, F. J. Vonk, R. A. Harrison, B. G. Fry, Complex cocktails: the
540 evolutionary novelty of venoms. *Trends Ecol. Evol.* **28**, 219–229 (2013).
- 541 2. Z. Nisani, W. K. Hayes, Defensive stinging by *Parabuthus transvaalicus* scorpions: risk
542 assessment and venom metering. *Anim. Behav.* **81**, 627–633 (2011).
- 543 3. S. Dutertre, *et al.*, Evolution of separate predation- and defence-evoked venoms in carnivorous
544 cone snails. *Nat. Commun.* **5**, 3521 (2014).
- 545 4. E. R. J. Evans, T. D. Northfield, N. L. Daly, D. T. Wilson, Venom costs and optimization in
546 scorpions. *Frontiers in Ecology and Evolution* **7** (2019).
- 547 5. S. D. Robinson, *et al.*, A comprehensive portrait of the venom of the giant red bull ant, *Myrmecia*
548 *gulosa*, reveals a hyperdiverse hymenopteran toxin gene family. *Sci Adv* **4**, eaau4640 (2018).
- 549 6. V. Schendel, L. D. Rash, R. A. Jenner, E. A. B. Undheim, The diversity of venom: The importance
550 of behavior and venom system morphology in understanding its ecology and evolution. *Toxins* **11**
551 (2019).
- 552 7. B. D. Blanchard, C. S. Moreau, Defensive traits exhibit an evolutionary trade-off and drive
553 diversification in ants. *Evolution* **71**, 315–328 (2017).
- 554 8. A. Touchard, *et al.*, The biochemical toxin arsenal from ant venoms. *Toxins* **8** (2016).
- 555 9. E. O. Wilson, B. Hölldobler, The rise of the ants: a phylogenetic and ecological explanation. *Proc.*
556 *Natl. Acad. Sci. U. S. A.* **102**, 7411–7414 (2005).
- 557 10. X. Cerdá, A. Dejean, Predation by ants on arthropods and other animals. *National Academy of*
558 *Sciences (US)* (2011).
- 559 11. D. B. Booher, *et al.*, Functional innovation promotes diversification of form in the evolution of an
560 ultrafast trap-jaw mechanism in ants. *PLoS Biol.* **19**, e3001031 (2021).
- 561 12. F. J. Larabee, A. V. Suarez, The evolution and functional morphology of trap-jaw ants
562 (Hymenoptera: Formicidae). *Myrmecol. News* **20**, 25–36 (2014).
- 563 13. J. Orivel, A. Dejean, Comparative effect of the venoms of ants of the genus *Pachycondyla*
564 (Hymenoptera: Ponerinae). *Toxicon* **39**, 195–201 (2001).
- 565 14. B. E. R. Rubin, S. Kautz, B. D. Wray, C. S. Moreau, Dietary specialization in mutualistic acacia-
566 ants affects relative abundance but not identity of host-associated bacteria. *Mol. Ecol.* **28**, 900–916
567 (2019).
- 568 15. C. Jelley, C. S. Moreau, Aggressive behavior across ant lineages: importance, quantification, and

- 569 associations with trait evolution. *Insectes Soc.* (2023).
- 570 16. D. C. Cardoso, Í. C. C. Alves, M. P. Cristiano, J. Heinze, Death feigning in ants. *Myrmecol. News*
571 **34** (2024).
- 572 17. D. A. Grasso, D. Giannetti, C. Castracani, F. A. Spotti, A. Mori, Rolling away: a novel context-
573 dependent escape behaviour discovered in ants. *Sci. Rep.* **10**, 3784 (2020).
- 574 18. V. Barassé, *et al.*, Venomics survey of six myrmicine ants provides insights into the molecular and
575 structural diversity of their peptide toxins. *Insect Biochem. Mol. Biol.* **151**, 103876 (2022).
- 576 19. A. Touchard, *et al.*, The complexity and structural diversity of ant venom peptidomes is revealed
577 by mass spectrometry profiling. *Rapid Commun. Mass Spectrom.* **29**, 385–396 (2015).
- 578 20. T. D. Kazandjian, *et al.*, Convergent evolution of pain-inducing defensive venom components in
579 spitting cobras. *Science* **371**, 386–390 (2021).
- 580 21. A. E. Mill, Predation by the ponerine ant *Pachycondyla commutata* on termites of the genus
581 *Syntermes* in Amazonian rain forest. *J. Nat. Hist.* **18**, 405–410 (1984).
- 582 22. A. Dejean, I. Olmsted, Ecological studies on *Aechmea bracteata* (Swartz) (Bromeliaceae). *J. Nat.*
583 *Hist.* **31**, 1313–1334 (1997).
- 584 23. B. Schatz, J. Orivel, J.-P. Lachaud, G. Beugnon, A. Dejean, Sitemate recognition: the case of
585 *Anochetus traegordhi* (Hymenoptera; Formicidae) preying on *Nasutitermes* (Isoptera: Termitidae).
586 *Sociobiology* **34**, 569–580 (1999).
- 587 24. A. Dejean, N. Labrière, A. Touchard, F. Petitclerc, O. Roux, Nesting habits shape feeding
588 preferences and predatory behavior in an ant genus. *Naturwissenschaften* **101**, 323–330 (2014).
- 589 25. T. Piek, *et al.*, Poneratoxin, a novel peptide neurotoxin from the venom of the ant, *Paraponera*
590 *clavata*. *Comp. Biochem. Physiol. C* **99**, 487–495 (1991).
- 591 26. A. Camargo, PCAtest: testing the statistical significance of Principal Component Analysis in R.
592 *PeerJ* **10**, e12967 (2022).
- 593 27. L. J. Revell, phytools: an R package for phylogenetic comparative biology (and other things).
594 *Methods Ecol. Evol.* **3**, 217–223 (2012).
- 595 28. C. Schmidt, Molecular phylogenetics of ponerine ants (Hymenoptera: Formicidae: Ponerinae).
596 *Zootaxa* **3647**, 201–250 (2013).
- 597 29. N. F. Carlin, D. S. Gladstein, The “bouncer” defense of *Odontomachus Ruginodis* and other
598 odontomachine ants (Hymenoptera: Formicidae). *Psyche* **96**, 1–19 (1989).
- 599 30. A. Dejean, *et al.*, The ecology and feeding habits of the arboreal trap-jawed ant *Daceton*
600 *armigerum*. *PLoS One* **7**, e37683 (2012).
- 601 31. E. Van Wilgenburg, M. A. Elgar, Colony characteristics influence the risk of nest predation of a
602 polydomous ant by a monotreme. *Biol. J. Linn. Soc. Lond.* **92**, 1–8 (2007).
- 603 32. A. De la Mora, G. Pérez-Lachaud, J.-P. Lachaud, Mandible strike: the lethal weapon of
604 *Odontomachus opaciventris* against small prey. *Behav. Processes* **78**, 64–75 (2008).
- 605 33. J. C. Gibson, F. J. Larabee, A. Touchard, J. Orivel, A. V. Suarez, Mandible strike kinematics of the
606 trap-jaw ant genus *Anochetus* Mayr (Hymenoptera: Formicidae). *J. Zool.* **306**, 119–128 (2018).
- 607 34. V. Barassé, *et al.*, Discovery of an insect neuroactive helix ring peptide from ant venom. *Toxins*
608 **15** (2023).
- 609 35. A. Touchard, *et al.*, Isolation and characterization of a structurally unique β -hairpin venom peptide
610 from the predatory ant *Anochetus emarginatus*. *Biochim. Biophys. Acta* **1860**, 2553–2562 (2016).
- 611 36. J. O. Schmidt, Pain and Lethality Induced by Insect Stings: An Exploratory and Correlational
612 Study. *Toxins* **11** (2019).
- 613 37. K. Kazuma, K. Masuko, K. Konno, H. Inagaki, Combined venom gland transcriptomic and venom
614 peptidomic analysis of the predatory ant *Odontomachus monticola*. *Toxins* **9**, 323 (2017).
- 615 38. J. Orivel, *et al.*, Ponericins, new antibacterial and insecticidal peptides from the venom of the ant
616 *Pachycondyla goeldii*. *J. Biol. Chem.* **276**, 17823–17829 (2001).
- 617 39. S. R. Johnson, J. A. Copello, M. S. Evans, A. V. Suarez, A biochemical characterization of the
618 major peptides from the Venom of the giant Neotropical hunting ant *Dinoponera australis*. *Toxicon*
619 **55**, 702–710 (2010).
- 620 40. S. Lv, *et al.*, Highly selective performance of rationally designed antimicrobial peptides based on
621 ponericin-W1. *Biomater Sci* **10**, 4848–4865 (2022).
- 622 41. A. S. Senetra, M. R. Necelis, G. A. Caputo, Investigation of the structure-activity relationship in
623 ponericin L1 from *Neoponera goeldii*. *Pept. Sci.* **112** (2020).

- 624 42. S. A. Nixon, *et al.*, Multipurpose peptides: The venoms of Amazonian stinging ants contain
625 anthelmintic ponericins with diverse predatory and defensive activities. *Biochem. Pharmacol.* **192**,
626 114693 (2021).
- 627 43. T. Jensen, *et al.*, Venom chemistry underlying the painful stings of velvet ants (Hymenoptera:
628 Mutillidae). *Cell. Mol. Life Sci.* **78**, 5163–5177 (2021).
- 629 44. A. A. Walker, *et al.*, Production, composition, and mode of action of the painful defensive venom
630 produced by a limacodid caterpillar, *Doratifera vulnerans*. *Proc. Natl. Acad. Sci. U. S. A.* **118**
631 (2021).
- 632 45. Z. Dekan, *et al.*, Δ -Myrtoxin-Mp1a is a helical heterodimer from the venom of the jack jumper ant
633 that has antimicrobial, membrane-disrupting, and nociceptive activities. *Angew. Chem. Weinheim*
634 *Bergstr. Ger.* **129**, 8615–8619 (2017).
- 635 46. S. R. Aili, *et al.*, An integrated proteomic and transcriptomic analysis reveals the venom complexity
636 of the bullet ant *Paraponera clavata*. *Toxins* **12** (2020).
- 637 47. S. D. Robinson, *et al.*, Ant venoms contain vertebrate-selective pain-causing sodium channel
638 toxins. *Nat. Commun.* **14**, 2977 (2023).
- 639 48. S. D. Robinson, *et al.*, Peptide toxins that target vertebrate voltage-gated sodium channels underly
640 the painful stings of harvester ants. *J. Biol. Chem.* **300**, 105577 (2024).
- 641 49. J. Pan, W. F. Hink, Isolation and characterization of myrmexins, six isoforms of venom proteins
642 with anti-inflammatory activity from the tropical ant, *Pseudomyrmex triplarinus*. *Toxicon* **38**,
643 1403–1413 (2000).
- 644 50. A. Touchard, *et al.*, Heterodimeric insecticidal peptide provides new insights into the molecular
645 and functional diversity of ant venoms. *ACS Pharmacol Transl Sci* **3**, 1211–1224 (2020).
- 646 51. P. A. Koenig, C. S. Moreau, Testing optimal defence theory in a social insect: Increased risk is
647 correlated with increased venom investment. *Ecol. Entomol.* (2023)
648 <https://doi.org/10.1111/een.13295>.
- 649 52. M. Hölzer, M. Marz, De novo transcriptome assembly: A comprehensive cross-species comparison
650 of short-read RNA-Seq assemblers. *Gigascience* **8** (2019).
- 651 53. Y. Xie, *et al.*, SOAPdenovo-Trans: de novo transcriptome assembly with short RNA-Seq reads.
652 *Bioinformatics* **30**, 1660–1666 (2014).
- 653 54. E. Bushmanova, D. Antipov, A. Lapidus, A. D. Prjibelski, rnaSPAdes: a de novo transcriptome
654 assembler and its application to RNA-Seq data. *Gigascience* **8** (2019).
- 655 55. M. G. Grabherr, *et al.*, Full-length transcriptome assembly from RNA-Seq data without a reference
656 genome. *Nat. Biotechnol.* **29**, 644–652 (2011).
- 657 56. M. Martin, Cutadapt removes adapter sequences from high-throughput sequencing reads.
658 *EMBnet.journal* **17**, 10–12 (2011).
- 659 57. B. E. R. Rubin, C. S. Moreau, Comparative genomics reveals convergent rates of evolution in ant–
660 plant mutualisms. *Nat. Commun.* **7**, 1–11 (2016).
- 661 58. R. Smith-Unna, C. Bournnell, R. Patro, J. M. Hibberd, S. Kelly, TransRate: reference-free quality
662 assessment of de novo transcriptome assemblies. *Genome Res.* **26**, 1134–1144 (2016).
- 663 59. F. A. Simão, R. M. Waterhouse, P. Ioannidis, E. V. Kriventseva, E. M. Zdobnov, BUSCO:
664 Assessing genome assembly and annotation completeness with single-copy orthologs.
665 *Bioinformatics* **31**, 3210–3212 (2015).
- 666 60. E. Bushmanova, D. Antipov, A. Lapidus, V. Suvorov, A. D. Prjibelski, rnaQUAST: a quality
667 assessment tool for de novo transcriptome assemblies. *Bioinformatics* **32**, 2210–2212 (2016).
- 668 61. B. J. Haas, *et al.*, De novo transcript sequence reconstruction from RNA-seq using the Trinity
669 platform for reference generation and analysis. *Nat. Protoc.* **8**, 1494–1512 (2013).
- 670 62. H. Nielsen, Predicting Secretory Proteins with SignalP. *Methods Mol. Biol.* **1611**, 59–73 (2017).
- 671 63. A. Krogh, B. Larsson, G. von Heijne, E. L. Sonnhammer, Predicting transmembrane protein
672 topology with a hidden Markov model: application to complete genomes. *J. Mol. Biol.* **305**, 567–
673 580 (2001).
- 674 64. B. Langmead, S. L. Salzberg, Fast gapped-read alignment with Bowtie 2. *Nat. Methods* **9**, 357–359
675 (2012).
- 676 65. B. Li, C. N. Dewey, RSEM: accurate transcript quantification from RNA-Seq data with or without
677 a reference genome. *BMC Bioinformatics* **12**, 323 (2011).
- 678 66. D. M. Bryant, *et al.*, A Tissue-Mapped Axolotl De Novo Transcriptome Enables Identification of

- 679 Limb Regeneration Factors. *Cell Rep.* **18**, 762–776 (2017).
- 680 67. S. Kumar, G. Stecher, M. Li, C. Knyaz, K. Tamura, MEGA X: Molecular Evolutionary Genetics
681 Analysis across Computing Platforms. *Mol. Biol. Evol.* **35**, 1547–1549 (2018).
- 682 68. A. M. Waterhouse, J. B. Procter, D. M. A. Martin, M. Clamp, G. J. Barton, Jalview Version 2—a
683 multiple sequence alignment editor and analysis workbench. *Bioinformatics* **25**, 1189–1191 (2009).
- 684 69. P. Dixon, VEGAN, a package of R functions for community ecology. *J. Veg. Sci.* **14**, 927–930
685 (2003).
- 686 70. R. R Core Team, Others, R: A language and environment for statistical computing (2013).
- 687 71. T. Galili, dendextend: an R package for visualizing, adjusting and comparing trees of hierarchical
688 clustering. *Bioinformatics* **31**, 3718–3720 (2015).
- 689 72. F. Teufel, *et al.*, SignalP 6.0 predicts all five types of signal peptides using protein language models.
690 *Nat. Biotechnol.* **40**, 1023–1025 (2022).
- 691 73. S. Ascoët, *et al.*, The mechanism underlying toxicity of a venom peptide against insects reveals
692 how ants are master at disrupting membranes. *iScience* **26**, 106157 (2023).
- 693 74. B. Q. Minh, *et al.*, IQ-TREE 2: New Models and Efficient Methods for Phylogenetic Inference in
694 the Genomic Era. *Mol. Biol. Evol.* **37**, 2461 (2020).
- 695